AD-A142 277 TRANSONIC SHOCK INTERACTION WITH A TANGENTIALLY-INJECTED TURBULENT BOUNDARY LAYER(U) WEST VIRGINIA UNIV MORGANTOWN G R INGER ET AL. JAN 84 N00014-81-K-0633 F/G 20/4 NL

1/ 1

UNCLASSIFIED

END

DATE FILMED

7-84

DTIC

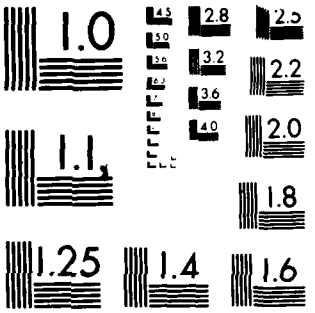

SECURITY CLASSIFICATION OF THIS PAGE (When Data Entered)

(12)

REPORT DOCUMENTATION PAGE

READ INSTRUCTIONS BEFORE COMPLETING FORM

1. REPORT NUMBER: AIAA-84-0094	2. GOVT ACCESSION NO.
3. RECIPIENT'S CATALOG NUMBER	
4. TITLE (and Subtitle): Transonic Shock Interaction with a Tangentially-Injected Turbulent Boundary Layer	5. TYPE OF REPORT & PERIOD COVERED: AIAA Paper 84-0094
	6. PERFORMING ORG. REPORT NUMBER
7. AUTHOR(s): G. R. Inger and A. Deane	8. CONTRACT OR GRANT NUMBER(s): N00014-81-K-0633; ONR NR-061-274
PERFORMING ORGANIZATION NAME AND ADDRESS: West Virginia University, Morgantown, WV 26506	10. PROGRAM ELEMENT, PROJECT, TASK AREA & WORK UNIT NUMBERS
CONTROLLING OFFICE NAME AND ADDRESS	12. REPORT DATE: Jan., 1984
	13. NUMBER OF PAGES: 16
MONITORING AGENCY NAME & ADDRESS (if different from Controlling Office): Office of Naval Research, 800 N. Quincy Street, Arlington, VA	15. SECURITY CLASS. (of this report): Unclassified
	15a. DECLASSIFICATION/DOWNGRADING SCHEDULE

DISTRIBUTION STATEMENT (of this Report)

Distribution Unlimited

DISTRIBUTION STATEMENT A
Approved for public release
Distribution Unlimited

17. DISTRIBUTION STATEMENT (of the abstract entered in Block 20, if different from Report)

Distribution Unlimited

DISTRIBUTION STATEMENT A
Approved for public release
Distribution Unlimited

18. SUPPLEMENTARY NOTES

DTIC ELECTE JUN 21 1984 S D B

19. KEY WORDS (Continue on reverse side if necessary and identify by block number)

Transonic Shock
Interaction
Turbulent
Tangential Injection

20. ABSTRACT (Continue on reverse side if necessary and identify by block number)

A non-asymptotic triple deck theory of transonic shock/turbulent boundary layer interaction is described which takes into account the influence of upstream tangential injection on a curved wall. In addition to Reynolds number and the shock strength, the theory is parameterized by arbitrary values of the incoming boundary layer shape factor, wall jet maximum velocity ratio and the nondimensional height of this ratio; results of a comprehensive parametric study are then presented. It is shown that the wall jet effects significantly reduce both the streamwise scale and displacement thickening of the interaction

DD FORM 1 JAN 73 1473

SECURITY CLASSIFICATION OF THIS PAGE (When Data Entered)

zone. While increasing the upstream and downstream skin friction levels, these effects also reduce the minimum interactive Cf and thus hasten the onset of incipient separation at the shock foot.

AIAA'84

AIAA-84-0094
Transonic Shock Interaction with a Tangentially-Injected Turbulent Boundary Layer

G.R. Inger and A. Deane, West Virginia Univ., Morgantown, WV

AIAA 22nd Aerospace Sciences Meeting

January 9-12, 1984/Reno, Nevada

TRANSONIC SHOCK INTERACTION WITH A TANGENTIALLY-INJECTED TURBULENT BOUNDARY LAYER

G. R. Inger[+] and A. Deane[++]
West Virginia University, Morgantown, W. Va.

Abstract

A non-asymptotic triple deck theory of transonic shock turbulent boundary layer interaction is described which takes into account the influence of upstream tangential injection on a curved wall. In addition to Reynolds number and the shock strength, the theory is parameterized by arbitrary values of the incoming boundary layer shape factor, wall jet maximum velocity ratio and the non-dimensional height of this ratio; results of a comprehensive parametric study are then presented. It is shown that the wall jet effects significantly reduce both the streamwise scale and displacement thickening of the interaction zone. While increasing the upstream and downstream skin friction levels, these effects also reduce the minimum interactive C_f and thus hasten the onset of incipient separation at the shock foot.

Nomenclature

A	Van Driest-Cebeci wall turbulence damping parameter
C_f	skin friction coefficient, $2\tau_w / \rho_{e_o} U_{e_o}^2$
ΔC_f	skin friction increment due to wall jet
C_p	pressure coefficient, $2 p' / \rho_{e_o} U_{e_o}^2$
C_ℓ	lateral spreading factor of wall jet
H^*	boundary layer shape factor, δ^*/θ^*
H_1	incompressible shape factor
K	curvature of wall in interaction region
M	Mach number
p	static pressure
p'	interactive pressure perturbation, $p-p_1$
Δp	pressure jump across incident shock
Re_x, Re^δ	Reynolds numbers based on length x and boundary layer thickness, respectively
S_w	non-dimensional wall shear function of wall jet
T	absolute temperature
$\bar{V}$	basic interactive wall-turbulence parameter
u',v'	streamwise and normal interactive disturbance velocity components, respectively
ΔU	wall jet component of total velocity profile
U_o	undisturbed incoming boundary layer velocity in x-direction
x,y	streamwise and normal distance coordinates (origin at the inviscid shock intersection with the wall)
$y_{w_{eff}}$	effective wall shift seen by interactive inviscid flow
y_{max}	location of ΔU_{max}
β	$\sqrt{M_1^2-1}$
γ	specific heat ratio
δ	boundary layer thickness
δ^*	boundary layer displacement thickness
δ_{mix}	wall jet mixing thickness
δ_{SL}	inner deck sublayer thickness
ϵ_T,	kinematic turbulent eddy viscosity
ϵ_T'	interactive perturbation of turbulent eddy viscosity
η	y/δ
μ	ordinary coefficient of viscosity
ν	μ/ρ
ω	viscosity-temperature dependence exponent, $\mu \sim T^\omega$
ρ	density
θ^*	boundary layer momentum thickness
τ	total shear stress
τ'	interactive perturbation of total shear stress

Subscripts

AD	adiabatic wall
1	undisturbed inviscid values ahead of incident shock
e	conditions at the boundary layer edge
inc	incompressible value
inv	inviscid disturbance solution value
max	velocity profile maximum due to wall jet
o	undisturbed incoming boundary layer properties

1. Introduction

The use of tangential slot-injection to influence and control turbulent boundary layer behavior has been extensively studied in various types of lowspeed external and internal aerodynamic flow fields (e. g., on circulation-controlled airfoils, slotted slaps, in film cooling applications and for separation control in inlets and diffusers). In recent years, many applications of such injection have arisen in supercritical transonic flow fields where local shock wave is present; however, little is presently available to provide a basic understanding of how the resulting shock-boundary interaction ("SBLI") alters the influence of tangential injection. Conversely, in such supercritical flows it may be of interest to know how the effects of SBLI may be altered by the use of injection. The present paper addresses these questions for the case of steady non-separating 2-D turbulent boundary layers on adiabatic surfaces of small-to-moderate longitudinal curvature.

The primary objectives of our work are to develop a fundamental theory of a transonic SBLI region occurring downstream of a tangentially-injected turbulent boundary layer on a curved wall (Fig. 1) and then to present the results of a parametric study of this theory showing the

[+] Professor and Associate Chairman, Dept. of Mechanical and Aerospace Engineering
[++] Graduate student.

relationship between the dominant physical parameters, the injection and the physics of the SBLI zone. In Section 2, we briefly outline the nonasymptotic triple deck theory of a SBLI zone on a curved surface without tangential injection. Then by taking the SBLI zone sufficiently far downstream of the injection slot for mixing of the wall jet and overlying turbulent boundary layer to have produced a well-defined "jet-bulged" boundary layer profile, the interactive perturbation field caused by normal shock interaction with this profile is analyzed in Section 3 by an extension of the aforementioned SBLI theory. This is followed in Section 4 by presentation and discussion of the results of a parametric study of this extended solution for the interactive pressure, displacement thickness and skin friction effects.

2. Brief Outline of the Basic SBLI Theory

2.1) The Triple-Deck Model

It is well-known experimentally that when separation occurs, the disturbance flow pattern associated with normal shock-boundary layer interaction is a very complicated one involving a bifurcated shock pattern[1], whereas the unseparated case pertaining to turbulent boundary layers up to $M_1 = 1.3$ has instead a much simpler type of interaction pattern which is more amenable to analytical treatment (Fig. 2). The flow consists of a known incoming isobaric turbulent boundary layer profile $M_o(y)$ subjected to small transonic perturbations due to an impinging weak normal shock. In the practical Reynolds number range of interest here [$Re_L \sim 10^7$ to 10^9] we purposely employ a nonasymptotic triple-deck flow model[2] in the turbulent boundary layer patterned after the Lighthill-Stratford-Honda approach that has proven highly successful in treating a variety of other problems involving turbulent boundary layer response to strong rapid adverse pressure gradients and which is supported by a large body of transonic and supersonic interaction data. The resulting flow model, Fig. 2, consists of an inviscid boundary value problem surrounding a shock discontinuity and underlaid by a thin shear stress-disturbance sublayer that contains the upstream influence and skin friction perturbations. An approximate analytic solution is further achieved by assuming small linearized disturbances ahead of and behind the nonlinear shock jump plus neglect of the detailed shock structure within the boundary layer, which give accurate predictions for all the properties of engineering interest when $M > 1.05$. The resulting equations can be solved by operational methods yielding the interactive pressure rise, displacement thickness growth and the skin friction behavior upstream and downstream of the shock foot. This solution contains all the essential global features of the mixed transonic viscous interaction flow and detailed comparisons with experiment[3,4] and Navier-Stokes numerical solutions have shown that it gives a very good account of all the important engineering features of non-separating interactions over a wide range of Mach-Reynolds number conditions.

An important and unique feature of this interaction theory is that it employs for the incoming turbulent boundary layer velocity profile a very general Composite Law of the Wall-Law of the Wake profile model due to Walz[5], which is characterized not only by the shock Mach number, M_1 and the boundary layer thickness Reynolds number Re_{δ^*} but also by arbitrary nonequilibrium values of the incompressible shape factor H_{i_1}. The resulting predictions, such as typically illustrated in Fig. 3, show that H_{i_1} has a very large effect on the local and downstream interactive properties that is important to account for in practical applications. By thereby accomodating a wide range of possible upstream histories of pressure gradient, heat and mass transfer, the theory has found wide-spread success as an interactive module in global composite viscous-inviscid flow field analysis programs on supercritical airfoils and projectiles, while also proving adaptable to the accomodation of new effects.

2.2) Wall Curvature and Shock Obliquity Effects

Since SBLI with tangential injection often arises in flows on curved surfaces, it is desireable to account for wall curvature effects in the foregoing interaction theory. For the small to moderate curvatures usually encountered ($K\delta_o^* \lesssim .02$), details analysis[6] of the transonic small disturbance flow in the outer deck shows that while the explicit new curvature terms in the perturbation equations are of the negligible order $K\delta_o^*$, the interactive viscous displacement effect from the underlying decks eliminates the well-known[7] inviscid shock singularity while slightly altering the shock into an oblique configuration. Detailed examination of the middle-deck region shows that any new terms in the inviscid rotational disturbance equations are of the negligible order $K\delta_o^*$; only the curvature effect on the undisturbed boundary-layer velocity and eddy viscosity profiles are of possible significance. Here again, the explicit $K\delta_o^*$ terms in the governing equations of this incoming flow are all negligible; however, curvature can moderately influence (10-20%) the eddy viscosity terms, with a consequent effect on the boundary-layer profile in the form of a skin friction reduction and shape factor increase as described approximately by the relationships[8]

$$C_{f_o} = (1 - 10K\delta_o^*)[C_{f_o}]_{flat} \qquad (1)$$

$$H_{i_1} = (1 + 5K\delta_o^*)[H_{i_1}]_{flat} \qquad (2)$$

where to this order of accuracy the corresponding effect on C_{f_o} is negligibly small. Note, for example, that the typical value $K\delta_o^* = 0.01$ yields a reduction and increase in C_{f_o} and H_{i_1} of 10 and 5%, respectively. The use of Eqs. (1) and (2) with the Walz velocity profile model and $K\delta_o^*$ as an additional input parameter provides a good engineering account of the moderate curvature effects on the middle-deck interaction solution. Within the very thin inner disturbance shear stress deck it is found yet again that the explicit curvature effects on the various inertia, pressure gradient, and laminar viscous terms in the disturbance flow equations are altogether negligible. Moreover, because of the extreme inner-deck thinness, the eddy viscosity curvature effect[9] therein can also be safely neglected for the high Reynolds number conditions typifying most practical external aerodynamic flows.

Predictive results for the typical influence of $K\delta_o$ on SBLI properties, which agree with experimental observations, may be found in Ref. 6; they show that the curvature effect slightly spreads out the interaction, weakening the adverse pressure gradient along the wall, due primarily to the increased shape factor. Since the curvature effect slightly reduces the incoming boundary-layer velocity profile fullness and spreads out the interaction, it further acts to thicken the downstream boundary layer while slightly increasing the local C_f around the shock foot owing to the reduced interactive pressure gradient. As regards the slight shock obliquity at the boundary layer edge caused by the interactive displacement thickness effect, detailed investigation[10] has established that it corresponds with a good approximation to the condition of "maximum" deflection. Hence the pressure rise is equivalent to a normal shock at the effective lower shock Mach number

$$M_{1_{eff}} = M_1 \sin\left(90^\circ - 37.3\sqrt{M_1 - 1}\right) \qquad (3)$$

thereby allowing the obliquity effect to be accurately accomodated in the present theory[11] (Fig. 4).

4. Extension to Include Tangential Injection

We recall that the aforementioned interaction theory feeds upon a known shock strength and an assumed incoming turbulent velocity profile model characterized by the overall parameters H_{i_1}, C_{f_o} and Re_{δ^*}. In the problem at hand we have a new unique shape of velocity profile that exists due to tangential blowing. In this section we will be concerned with modeling such a profile and its associated wall-region eddy viscosity behavior by a convenient set of parameters that characterize the essential new physical features and yet are flexible enough to accomodate later specific data and to allow parametric sensitivity studies.

When air is tangentially injected through a slot of height h into an overlying boundary layer it forms a jet which is entrained by the surrounding flow (Fig. 5a). Immediately downstream of the slot, strong mixing of these flows occurs in a complicated manner which may not be validly treated by boundary layer theory; in any event, the resulting composite velocity profile assumes a unique character with a maximum and a minimum (Fig. 5b). As the flow proceeds further downstream, experimental studies[12] have shown that the minimum is rapidly eliminated by further mixing so that when $x \gg h$, the profile attains a fully-developed "jet-bulged" shape (Fig. 5c) composed of an unblown-type of turbulent boundary layer profile plus a wall jet component containing a velocity maximum near the wall. As this fully-developed shape convects downstream, further mixing gradually decreases and spreads out the jet maximum (Fig. 5d) until the boundary layer ultimately tends toward an ordinary monotone profile shape in which the jet component has been completely eliminated by entrainment. In the present study of weak transonic normal shock interaction with the boundary layer downstream of a tangential injection slot, we will deal with the case where the shock interacts with a "jet-bulged" type of profile (Fig. 5c); this is the most interesting encountered in practice.*

While possessing a boundary layer profile shape that can be analytically modeled in a manner appropriate to the SBLI solution (see below), this case also permits a simplified treatment of the eddy viscosity aspects of the interactive decks in the boundary layer, as follows. Experimental studies[12-14] have shown that the usual Law of the Wall behavior and its associated mixing length eddy viscosity model applies to the lower portion below the jet maximum when the injection effect is small-to-moderate ($\Delta u_{max}/u_e \gtrsim 1.0$). Since the thin disturbance-shear stress inner deck of the SBLI region lies well within this Law of the Wall region, while there are no eddy viscosity-associated perturbation terms in the overlying middle deck owing to the inviscid frozen-turbulence nature of its disturbance flow, height, it can be shown that the form of all the basic triple-deck Equations in the aforementioned SBLI theory can be carried over to the present problem provided that one fully accounts for the wall jet effects on the undisturbed flow skin friction C_{f_o}, displacement thickness Reynolds number Re_{δ^*} and (especially) incompressible shape factor H_{i_1} as well as the profile distribution itself.

An appropriate analytical model of the incoming boundary layer profile was developed which accounts for the essential new wall-jet features of the flow while also being well-suited to the Lighthill pressure disturbance equation that is involved in the middle deck solution. It is constructed as the sum of a wall-jet component and an "unblown" component, where to be consistent with earlier work the latter is represented by Wild's Law of the Wall Law of the Wake composite profile characterized by the three parameters Re_{δ^*}, C_{f_o} and H_{i_1} (see Appendix A). Thus if y_{max} denotes the height of the maximum velocity u_{max} with Δu_{max} denoting the corresponding difference between u_{max} and the unblown velocity due to the wall jet effect (see Fig. 6), the total profile is expressed as

$$u(y) = u_{wallz}(y) + \Delta u(y) \qquad (4)$$

where the wall jet component $\Delta u(y)$ varies from zero at $y = 0$ (no slip) to its maximum value Δu_{max} at $y = y_{max}$ and then decays outwardly towards zero, becoming negligible beyond some characteristic jet-spread height δ_{mix} above y_{max} (we presume $\delta_{mix} + y_{max} \ll \delta$). Above y_{max}, we have followed the experimentally-based work of Carrière et al[15] and represented Δu by a modified sech^2 function whose slope at y_{max} equals $-(du_{wallz}/dy)_{y_{max}}$ such that the total composite profile correctly has a maximum at y_{max}:

$$\frac{\Delta u}{u_e} = \frac{\Delta u_{max}}{u_e}\left\{\frac{\text{SECH}^2\left[\left(\frac{y - y_{max}}{\delta_{mix}}\right) + \$\right]}{\text{SECH}^2\$}\right\} \qquad (5)$$

*The regions upstream of the slot and very far downstream where the profile maximum has disappeared can of course be handled by the existing "unblown" version of the present SBLI theory.

where

$$\ddagger = \tfrac{1}{2}\left[\ln\left(1 + \frac{C_x}{2}\right) - \ln\left(1 - \frac{C_x}{2}\right)\right] \qquad (5B)$$

is a phasing factor insuring the maximum in total velocity at y_{max} and

$$C_x = (\delta_{mix}/\Delta U_{max})\left[\partial \Delta u/\partial y\right]_{max}$$

is a lateral spreading constant (typically = .15 to avoid secondary profile maxima above y_{max}).

Below y_{max}, on the other hand, we require a functional representation that gives a reasonable monotonic shape and matches smoothly to Eq. (5) at y_{max}. Furthermore, we desire some control over the wall slope in order to represent injection effects on the local skin friction ΔC_f. The specific constraints on this functional choice are (a) only one maximum in the total composite profile at $y = y_{max}$, (b) a match with the value and slope of the upper $\Delta u(y)$ function at y_{max}, and (c) positive values of the non-dimensional slope

$$S_w \equiv \left[\frac{d(\Delta u/u_e)}{d(y/y_{max})}\right]_{y=0}$$

leading to physically reasonable skin friction increments

$$C_f = S_w\,(\mu_w \delta^*/\mu_e Re_\delta)\,\Delta U_{max}/y_{max} \qquad (6)$$

Now condition (a) so severely restricts the class of monotone functions it admits that no general solution can be generated to accommodate a completely arbitrary combination of conditions (b) and (c); what can be found, however, are functions which allow either an arbitrary choice of all three parameters S_w, ΔU_{max}, y_{max} within a restrictive range or the choice of a wide range of values for the two key parameters ΔU_{max}, y_{max} with S_w then consequently determined (but still within an interesting range of resulting values). One such function which has proven quite satisfactory for the purposes of this investigation is

$$\frac{\Delta u}{u_e} = C_1 \frac{y}{y_{max}} - C_3\left[\exp\left(C_2 \frac{y}{y_{max}}\right) - 1\right]$$

$$(y < y_{max}) \qquad (7A)$$

where the aforementioned matching conditions are fulfilled if the constants $C_{1,2,3}$ satisfy the three simultaneous relations

$$C_1 - C_3\,(\exp C_2 - 1) = \Delta u_{max} \qquad (7B)$$

$$C_1 - C_3 C_2 \exp C_2 = -\,y_{max} \qquad (7C)$$

$$C_1 - C_3 = S_w \qquad (7D)$$

This trio is readily solved numerically during the implementation of the velocity profile model by using a standard non-linear simultaneous root-finder subroutine.

The aforementioned provides a smooth, piecewise-continuous and physically realistic analytical model of a fully-turbulent boundary layer downstream of a tangential injection slot; it captures the velocity overshoot and negative vorticity region features unique to this kind of flow (Fig. 6) while containing sufficient basic parameterization to permit sensitivity studies of how the jet-bulge effect influences the SBLI zone. Moreover, it has the advantage of allowing current and later experimental data on turbulent wall-jet boundary layer behavior to be incorporated into the interaction study without tying the present research down to the much more difficult and lengthy effort of such experimental studies. The weak boundary layer compressibility effects on this profile for adiabatic transonic flow are quite satisfactorily accounted for by the reference temperature method.[16]

3.2) Implementation of the Extended Theory

The foregoing approach may be implemented by several straightforward modifications to the existing computer program for the zero-blowing SBLI theory, as follows. To include small-to-moderate wall curvature effects ($K\delta_o < .01$), we add $K\delta_o$ as an independent input variable and accordingly modify the input values of H_{i_1} and Cf_o according to Eqs. (1) and (2); furthermore, we eliminate the inviscid curvature singularity, altering the normal shock to a slightly oblique one at the boundary layer edge, by modifying the input effective normal shock Mach number according to Eq. (3). The influence of tangential injection is accomodated by introducing the two new input parameters $\Delta U_{max}/U_e$ and y_{max}/δ_o, characterizing the magnitude and height, respectively, of the wall jet component effect; in addition, values of the auxillary parameters C_x and S_w can be set within certain restricted ranges.† The program subroutine which evaluates the Walz turbulent boundary layer velocity profile model is modified to add the matched upper and lower wall jet-component increments pertaining to these inputs (Eqs. 4-7), using a Reference Temperature-Method compressibility correction of the appropriate parameters. Figure 7 illustrates some typical boundary layer velocity profiles containing these tangential injection effects. Using the adiabatic temperature-velocity relationship

$$T = T_{W,AD} + (T_e - T_{W,AD})\,U^2/U_e^2 \qquad (8)$$

the associated Mach number profile $M_o(y)$ and its derivative dM_o/dy (which are both needed in the subsequent SBLI solution routine) are calculated, the corresponding mass flow and momentum defect distributions $1 - \frac{\rho u}{\rho_e U_e}$ and $\left(1 - \frac{\rho u}{\rho_e U_e}\right)\frac{u}{u_e}$ are also integrated across the boundary layer to obtain the values of δ^*/δ and θ^*/δ, respectively, associated with the wall jet effect. The resulting values of the displacement thickness and shape factor are shown in Figs. 8A and 8B, to illustrate how the mass and momentum addition to the boundary layer from the wall jet substantially decreases δ^* and produces a greater profile "fullness", reflected in a significantly reduced shape factor.† Increasing

† It is formally possible to obtain negative δ^* and θ^* for sufficiently large injection rates (ΔU_{max}, say); consistent with our other assumptions, however, we exclude such cases from this study.

the height of the jet maximum is seen to have a similar effect, because this enhances the effective strength of the injection effect on the boundary layer profile. Awareness of these overall integral property effects proves helpful in interpreting the predicted interaction properties given below.

Implementation of these wall jet-modifications is quite straightforward, except to note that feedback of the aforementioned modified integral properties into the solution sequence must be properly phased: since the wall jet effect on the incoming boundary layer profile shape is already included in the $M_o(y)$ distribution used in solving the Lighthill interactive pressure equation, the feedback must be done after this pressure disturbance solution is carried out. Subsequent use of the jet-altered values of δ^* and Cf_o then further influences the local interactive displacement thickening and skin friction solution results. To illustrate the importance of this proper feedback of the jet-influenced profile integral properties a typical set of interactive pressure, displacement thickness and skin friction distributions predicted by the aforemetioned extended theory are presented in Fig. 9, showing the various relative effects of tangential injection compared to the zero blowing case. It is seen that the increased boundary layer profile fullness and shape factor reduction due to injection causes a significant streamwise contraction of the interactive pressure rise; this is in agreement with experimental observations (see, e.g., Fig. 116, p. 1323 of Ref. 17). Accompanying this contraction of the interaction zone, the two main effects of injection on the ratio $\Delta\delta^*/\delta_o^*$ are seen to act with opposite and nearly equal influence: while the profile shape-factor effect of injection reduces $\Delta\delta^*$, the corresponding reduction of δ_o^* is approximately of the same magnitude so that the overall change in $\Delta\delta^*/\delta_o^*$ is small. This implies that the net injection effect on $\Delta\delta^*$ scales approximately with the corresponding effect on δ_o^*. Turning to the interactive skin friction behavior typified in Fig. 9c, it can be seen that the increased Cf level due to the wall jet effect dominates most of the interaction zone both fore and aft of the shock except in the vicinity of the shock foot; in this foot region, the Cf reduction due to the steepened interactive pressure gradient caused by injection becomes the dominant effect and the local value of Cf_{min} is actually reduced. Stated another way, the SBLI effect adversely counteracts the otherwise favorable Cf increase due to injection.

The aforementioned tangential injection effects on SBLI may be readily understood from the overall shape factor and displacement thickness effects shown in Fig. 8: the reduced H and δ^* imply a thinner incoming turbulent boundary layer with a somewhat higher Mach number deep in the layer and a fuller profile shape typical of a favorable upstream pressure gradient history, which in view of the demonstrated sensitivity of SBLI to the shape factor (Fig. 3) have the effect of reducing the streamwise scale and interactive thickening while increasing the corresponding local pressure gradient.

3.3) Imbedded Regions of Negative Vorticity and Supersonic Flow in the Boundary Layer

It has been seen that the wall jet effect results in a strata of negative vorticity flow above the maximum deep down in the incoming boundary layer profile (Fig. 6). Now, some earlier basic studies of shock interaction with idealized shear flows (simple velocity discontinuities) suggest that such a strata of vorticity sign reversal might significantly alter the character of the shock transmission and reflection across it, in turn implying possible difficulty with the numerical solution across this strata of the Lighthill[18] interactive pressure disturbance equation in the present SBLI theory (which involves a term $\sim \partial p/\partial y \cdot dU_o/dy$). We therefore examined this point carefully, with the following reassuring conclusion: provided that reasonable care is taken to insure high numerical accuracy with an appropriately smaller step size Δy, the Lighthill equation solution is quite regular for any smooth albeit rapid variation in sign (dM_o/dy) across the strata. Hence the overall interaction solution is modified, but not fundamentally altered, by the presence of the negative vorticity due to the wall jet effect and this is straightforwardly accounted for by our modified velocity profile model in the Lighthill equation and by the associated change of the integral parameters. The underlying reason for this lack of difficulty with rapid local variations in either magnitude or sign of dM_o/dy may be found from an analysis of the large scale features of Lighthill's equation, which reveals that its solution essentially depends only on integrals, rather than on local details, of the $M_o(y)$ distribution across the boundary layer.

The presence of a local velocity maximum deep within the boundary layer also raises another possible difficulty, when the wall jet effect is sufficiently large, associated with the existence of a strata of locally supersonic flow astride the velocity maximum (Fig. 10). When this occurs, it is seen that there are two special cases where dM_o/dy vanishes at a sonic point within the boundary layer and where a local transonic singularity in the Lighthill pressure equation solution therefore will occur: (a) at a tangential injection rate where U_{max} just goes sonic, and (b) at a slightly higher rate where the local minimum U goes sonic higher up in the boundary layer. In these two isolated cases, there is a local breakdown of the linearization underlying the Lighthill equation and the resulting transonic singularity which causes fundamental difficulties with the numerical solution of this equation that can only be cured by restoring (at least locally) the appropriate non-linear transonic correction term. For all other maximum wall jet velocities (including, interestingly enough, the so-called "overblown" cases where $M_{max} > M_e$), the boundary layer contains only one local sonic point that is well-removed from $dM_o/dy = 0$ (for subsonic U_{max} it lies above y_{max} while for supersonic U_{max} it lies below). In such normal cases, no fundamental difficulties were discerned.

4. Discussion of Parametric Study Results

The present theory has been used to carry out a systematic study of how the key tangential injection parameters influence the essential properties of a subsequent SBLI zone. We now present and discuss the results.

4.1) Interactive Pressure and Displacement Thickening

Typical pressure distributions, showing the strong systematic contraction of the streamwise interactive scale with increasing strength of the wall jet component-effect, are illustrated in Figure 11. A comprehensive summary of such results showing the upstream and downstream influence distances (the distance ahead and behind the shock where the pressure rise is 5% and 95%, respectively, of the overall shock jump value) are presented in Figures 12 and 13 as a function of both the magnitude and location of the jet velocity maximum for a typical supercritical flow of $M_1 = 1.20$. Additional plots showing the influence of the incoming (unblown) shape factor, shock strength and Reynolds number on the wall jet effects are presented in Figures 14-17. Taken overall, these results show that tangential injection can significantly reduce the overall upstream influence, and strongly reduce the downstream streamwise scale of the interaction to a degree comparable to, or greater than, the unblown shape factor and/or Mach number effects. When non-dimensionalized in terms of δ_o, the results are not very sensitive to Reynolds number.

The corresponding systematic influence of injection on the relative interactive displacement thickness distribution $\delta\delta^*(x)/\delta_o^*$ is illustrated in Figure 18, where we see that the effect on $\delta\delta^*(x)$ and δ_o^* largely cancel over a wide range of wall jet strengths when presented in this ratioed manner. However, there is a significant injection effect on the streamwise slope of $\Delta^*(x)$ at the shock foot, which relates to the effective "viscous wedge" angle sensed by the outer inviscid flow; this effect is illustrated in Fig. 19, where the strong increase of this slope with wall jet strength may be clearly seen.

4.2) Incipient Separation

The present theory, although it breaks down at separation, *does yield a useful indication of incipient separation* where $Cf_{min} \to 0$, owing to the particular attention paid to the treatment of the local interactive skin friction behavior. Since this indication is of great practical interest, a parametric study of incipient separation conditions inherent in the present theory was carried out.

As a basis for comparison, the results for flow without any tangential injection are shown in Fig. 20a where the shock Mach number above which incipient separation occurs is plotted as a function of the Reynolds number with the shape factor as a parameter; also shown in the figure is the approximate experimental boundary determined by a careful examination of a large number of transonic interaction tests, besides Nussdorfer's[19] $M \sim 1.30$ criterion for turbulent flow. It is seen that the theoretical prediction of a gradual *increase in the incipient separation* Mach number value with Revnolds number is in agreement with the trend of this data. The theoretical prediction of only a small influence of shape factor on the incipient separation conditions is also borne out by more recent data[20] as indicated in Fig. 20b. We note here that the absolute values of the incipient separation Mach number predicted on the basis of a normal shock are consistently underpredicted slightly (Fig. 20a): when the shock obliquity effect is modeled as described above, it is seen that the present theory and experiment are in *good agreement* over a wide range of Reynolds numbers.

Turning to the effect of injection, we first note from the typical behavior of the interactive Cf *distribution around the shock foot (see, e.g., Fig. 9c)* that the net effect is expected to decrease Cf_{min} (notwithstanding the overall upstream and downstream increase in Cf otherwise due to injection). As shown in Fig. 21, this is indeed found to be the case: the wall jet effect of increasing the local interactive pressure gradient is seen to hasten the onset of incipient separation at the shock foot for a given Reynolds number flow; in the sense that separation occurs at a slightly lower shock number as $\delta U_{max}/U_e$ is increased. This is of course in sharp contrast to the well-known[17] favorable effect of injection in *delaying* separation observed for purely subsonic[21] flows with a prescribed adverse pressure gradient, and is due to the fact that the interactive pressure gradient enhancement effect of tangential injection in locally reducing Cf is absent in the latter flows.

4.3) Downstream Effects

The SBLI effect has been shown in several comprehensive studies[11,22] of supercritical airfoil flow fields to have an appreciable influence on both shock location and downstream boundary layer behavior, and hence a significant global aerodynamic influence, when the shock occurs downstream of 65-70% chord (Fig. 22). Therefore, the predicted influence of tangential injection on the post-interactive boundary layer properties would be of interest, as would the extent to which SBLI alters the injected boundary layer behavior that otherwise exists downstream.

Now, we have seen above that tangential injection reduces the SBLI displacement thickness growth while increasing the downstream post-interactive Cf (Fig. 9c). Alternatively, we may view SBLI as increasing the downstream δ^*, and hence counteracting the thinning effect otherwise obtained by the wall jet, while reducing the injection-produced Cf enhancement; both these SBLI effects make the boundary layer less resistant to separation in any subsequent adverse pressure gradient region it may encounter, and hence diminish the effectiveness of injection in otherwise delaying downstream separation. Regarding the skin friction, these conclusions are summarized in Fig. 23, where there is shown the typical influence of increasing wall jet strength on the post-interactive Cf: it is seen that while weak injection at first increases it slightly due to the corresponding increase in Cf_o, stronger injection rates have the opposite effect of lowering it (as well as Cf_{min}) because of the intensified adverse pressure gradient effect.

5. Concluding Remarks

Viewed overall, the present study has shown that the usual favorable tangential injection effects of thinning out and delaying the separation of turbulent boundary layers in subsonic flow can be significantly compromised by transonic

shock/boundary layer interaction. Conversely, such injection was seen to appreciably reduce the streamwise extent of an SBLI zone albeit with the allied consequence of intensifying the local interactive adverse pressure gradient and onset of shock foot separation. It has further been established that a fundamentally-based triple-deck theory of SBLI with injection is now available to treat these effects in either external or internal supercritical flow fields; moreover, this theory has been constructed to serve as a locally insertable interactive module astride the inviscid shock location, driven by the attendant local boundary layer properties including an arbitrary non-equilibrium shape factor. Consequently it would be possible to investigate in the future interesting problems of blowing in supercritical flow fields, including the use of tangential injection to modify the influence of SBLI upon the viscous trailing edge effect of supercritical airfoils[22,23] and the inclusion of SBLI effects in viscous-inviscid flow field analysis programs for circulation-controlled airfoils and wings flying at supercritical flight speeds.

Acknowledgement

This work was carried out under the auspices of Office of Naval Research Contract NR-061-274; the resulting support and encouragement of Dr. Robert Whitehead of ONR is sincerely appreciated.

Appendix

Because of its convenient analytical form, accurate blended representation of the combined Law of the Wall - Law of the Wake behavior and generality, we have adopted Walz's model[7] for the incoming turbulent boundary layer upstream of the intersection. For the low Mach number small heat transfer conditions appropriate to transonic interactions, it may be satisfactorily corrected for compressibility effects by the Eckert Reference Temperature method which under these conditions is, in fact, comparable in accuracy to, but far simpler to implement than, the Van Priest[24] compressibility transformation approach.

Let Φ be Coles' (incompressible) Wake Function $\Phi = y^+$ and denote for convenience $R \equiv .41\, Re^{\delta^*}_{\delta}\left[(1 + \tfrac{\gamma-1}{2} M_e^2)(T_w/T_e)\right]^{1+\omega}$ with $\omega = .76$ and $\gamma = 1.4$ for a perfect gas; then the compressible form of Walz's composite profile may be written

$$\frac{U_o}{U_e} = 1 + \frac{1}{.41}\sqrt{\frac{C_{f_o}}{2}\left(\frac{T_w}{T_e}\right)}\left[\left(\frac{R}{1+R}\right)\eta^2(1-\eta)-2\pi\eta^2(3-2\eta) + \ln\left(\frac{1+R\eta}{1+R}\right) - (.215 + .655R\eta)e^{-3R\eta}\right] \qquad (A\text{-}1)$$

subject to the following condition linking Π to C_{f_o} and $Re^{\delta^*}_{\delta}$:

$$2\pi + .215 + \ln(1+R) = \frac{.41}{\sqrt{\frac{C_{f_o}}{2}\left(\frac{T_w}{T_e}\right)}} \qquad (A\text{-}2)$$

Eqs. (A-1) and (A-2) have the following desirable properties: (a) for $\eta \geq .10$ or so U_o/U_e is dominated by a Law of the Wake behavior which correctly satisfied both the outer limit conditions $U_o/U_e \to 1$ and $dU_o/dy \to 0$ as $\eta \to 1$; (b) on the other hand, for very small η values, U_o assumes a Law of the Wall - type behavior consisting of a logarithmic term that is exponentially damped out extremely close to the wall into a linear laminar sublayer profile $U/U_e = R\eta$ as $\eta \to 0$; (c) Eq. (A-1) may be differentiated w.r.t. η to yield an analytical expression for dU_o/dy also, which proves advantageous in solving the middle and inner deck interaction problems (see text) where dM_o/dy must be known and vanish at the boundary layer edge.

The use of the incompressible form of Eq. (A-1) in the defining integral relations for δ_1^* and θ_1^* yields the following relationship that links the wake parameter to the resulting incompressible shape factor $H_{i_1} \equiv (\delta_1^*/\theta_1^*)_1$:

$$\frac{H_{i_1} - 1}{H_{i_1}} = \frac{2}{.41}\sqrt{\left(\frac{T_w}{T_e}\right)\frac{C_{f_o}}{2}}\left(\frac{1 + 1.59\pi + .75\pi^2}{1+\pi}\right) \qquad (A\text{-}3)$$

Eqs. (A-2) and (A-3) together with the defining relation for R enable a rather general and convenient parameterization of the profile (and hence the interaction that depends on it) in terms of three important physical quantities: the shock strength (M_{e_1}), the displacement thickness Reynolds number $Re^{\delta_1^*}$, the wall temperature ratio T_w/T_e and the shape factor H_{i_1} that reflects the prior upstream history of the incoming boundary layer including possible pressure gradient and surface mass transfer effects. With these parameters prescribed, the aforementioned three equations may be solved simultaneously for the attendant skin friction C_{f_o}, the value of R and, if desired, the π value appropriate to these flow conditions.

References

1. Ackeret, J. F. Feldman and N. Rott, "Investigation of Compression Shocks and Boundary Layers in Gases Moving at High Speed," NACA TN-1113, 1947.
2. Inger, G. R., "Upstream Influence and Skin Friction in Non-Separating Shock Turbulent Boundary Layer Interactions," AIAA Paper 80-1411, Snowmass, Colo., July 1980.
3. Inger, G. R., "Some Features of a Shock-Turbulent Boundary Layer Interaction Theory in Transonic Flow Field," AGARD CP-291, Symposium on Computation of Viscous-Inviscid Interactions, Colorado Springs, Colo., Sept. 1980, pp. 18-1 to 18-66.
4. Inger, G. R., "Application of a Shock-Turbulent Boundary Layer Interaction Theory in Transonic Flowfield Analysis", Ch. 17 of Transonic Aerodynamics, Vol. 81, Progress in Astronautics and Aeronautics, AIAA, 1982.
5. Walz, A., "Boundary Layers of Flow and Temperature," M.I.T. Press, Cambridge, Mass., 1969, pp. 113.
6. Inger, G. R., "Transonic Shock-Turbulent Boundary Layer Interaction and Incipient Separation on Curved Surfaces," AIAA Paper 81-1244, Palo Alto, June, 1981. Jour. of Aircraft 20, June 1983, pp. 571-74.
7. Oswatitsch, K., and J. Zierep, "Das Problem

des senkrechten Stosses an einer gekrummten Wand," ZAMM 40, 1960, pp. 143-147.

8. Bradshaw, P., "Effects of Streamline Curvature on Turbulent Flow," Agardograph 169, Aug. 1973.
9. Cebeci, T. "Wall Curvature and Transition Effects in Turbulent Boundary Layers", AIAA Jour. 9, Sept. 1971, 1868-1870.
10. Inger, G. R., and H. Sobieczky, "Shock Obliquity Effect on Transonic Shock-Boundary Layer Interaction," ZAMM 58T, 1978.
11. Nandanan, M., Stanewsky, E. and Inger, G. R., "A Computational Procedure for Transonic Airfoil Flow Including a Special Solution for Shock-Boundary Layer Interaction," AIAA Paper 80-1389, Snowmass, Colo., July 1980. AIAA J. Dec. '81, January 1982.
12. M. P. Escudier, W. B. Nicoll, D. B. Spalding, and J. M. Whitelaw, "Decay of a Velocity Maximum in a Turbulent Boundary Layer," Aero Quart. Vol. XVIII, Pt. 2, May 1967, pp. 121-132.
13. Dvorak, F. A., "Calculation of Turbulent Boundary Layers and Wall Jets Over Curved Surfaces," AIAA Jour. 11, April 1973, pp. 517-22.
14. Hubbartt, J. E. and D. H. Neale, "Wall Layer of Plane Turbulent Wall Jets Without Pressure Gradients", J. of Aircraft 9, March 1972, pp. 195-196.
15. Carriere, P., E. Eichelbrenner and Ph. Poisson-Quinton, "Contribution Theoretique et Experimentale a L'Etude du Controle de la Couche Limite par Soufflage," in Advances in Aeronautical Sciences, Vol. 2, Pergamon Press, 1959.
16. Burggraf, O. R., "The Compressibility Transformation and the Turbulent Boundary Layer Equation," Jour. of the Aerospace Sci. 24, 1962, pp. 434-439.
17. Chang, P. Control of Flow Separation, Pergamon Press, N.Y. 1972; p. 330-375, plus 1323.
18. Lighthill, M. J., "On Boundary Layers and Upstream Influence, II. Supersonic Flow with Separation," Proceedings of the Royal Society A, Vol. 217, 1953, pp. 478-507.
19. Nussdorfer, T. J., "Some Observations of Shock Induced Turbulent Separation on Supersonic Diffusors," NACA RM E51L26, May 1956.
20. Sirieix, M., J. Delery and E. Stanewsky, "High Reynolds Number Boundary Layer-Shock Wave Interaction in Transonic Flow", Lecture Notes in Physics, Springer-Verlag, 1982.
21. Burley, R. R., and D. P. Huang, "Experimental and Analytical Results of Tangential Blowing Applied to a Subsonic V/STOL Inlet," AIAA Paper 82-1084, June 1982.
22. Lekoudis, S. G., G. R. Inger and M. Khan, "Computation of the Viscous Transonic Flow Around Airfoils with Trailing Edge Effects and Proper Treatment of the Shock-Boundary Layer Interaction," AIAA Paper 82-0989, St. Louis, June, 1982.
23. Melnick, R. E., [illegible] and H. P. Mead, "Theory of Viscous Transonic Flow Over Airfoils at High Reynolds Number," AIAA Paper 77-683, June 1977.
24. Van Driest, E. R. "Turbulent Boundary Layers in Compressible Fluids," Jour. of the Aeronaut. Sci. 18, March 1951, pp. 145-160.

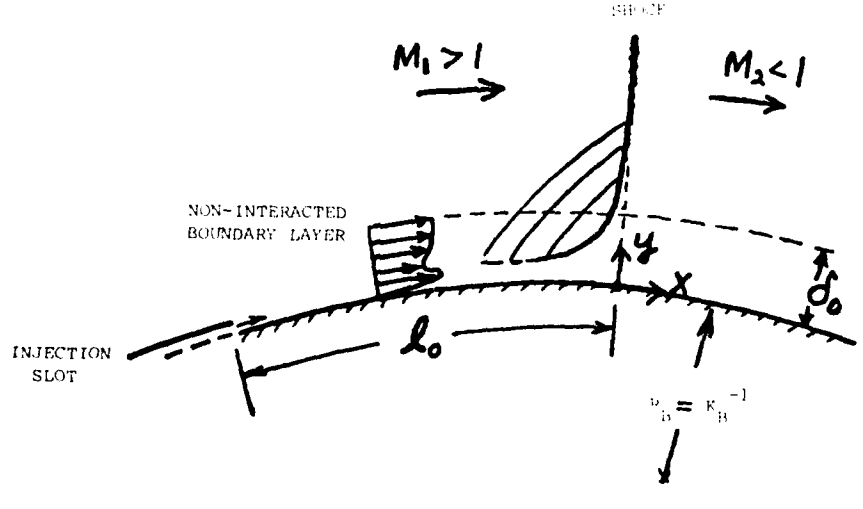

Fig. 1 Interaction Problem Configuration

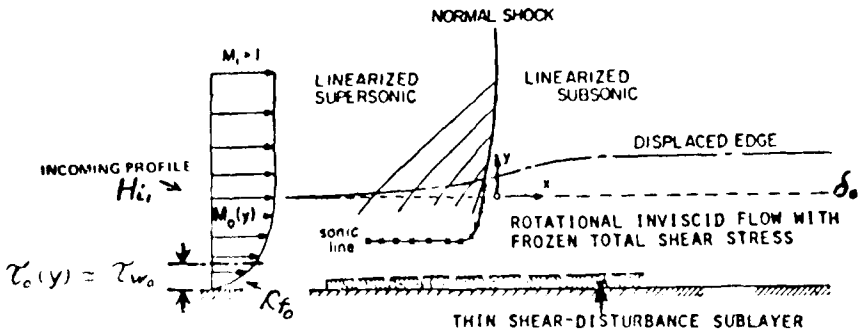

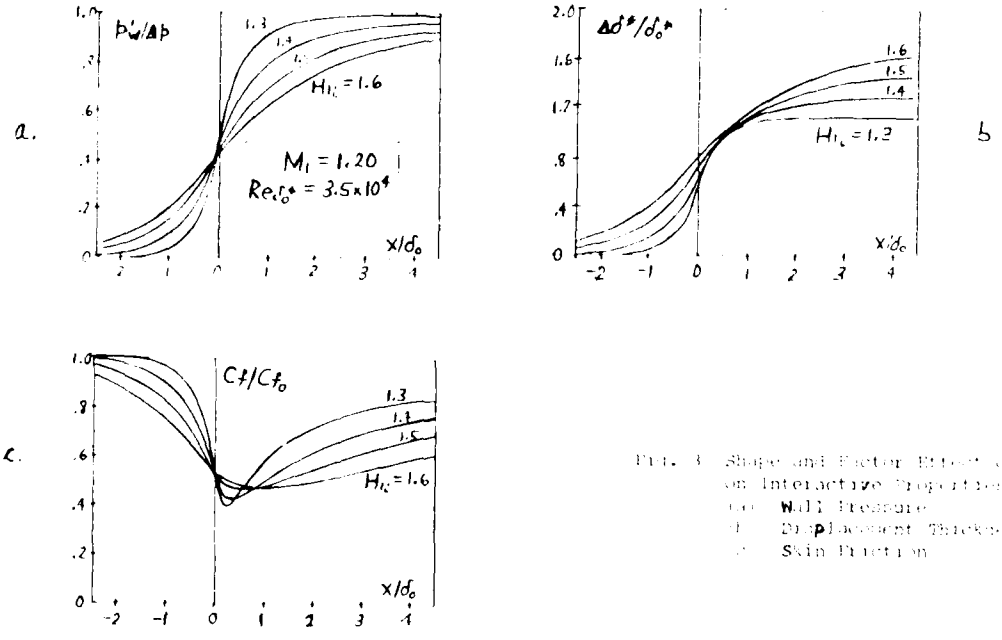

Fig. 3 Shape and Factor Effect on Interactive Properties
a. Wall Pressure
b. Displacement Thickness
c. Skin Friction

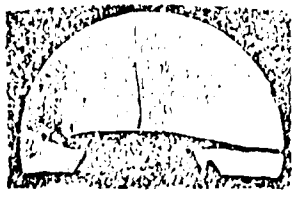

Fig. 4

Axisymmetry Effect due to Viscous Effects

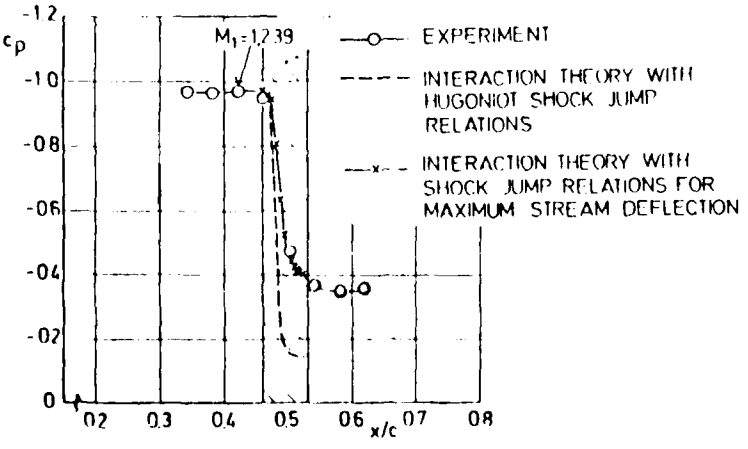

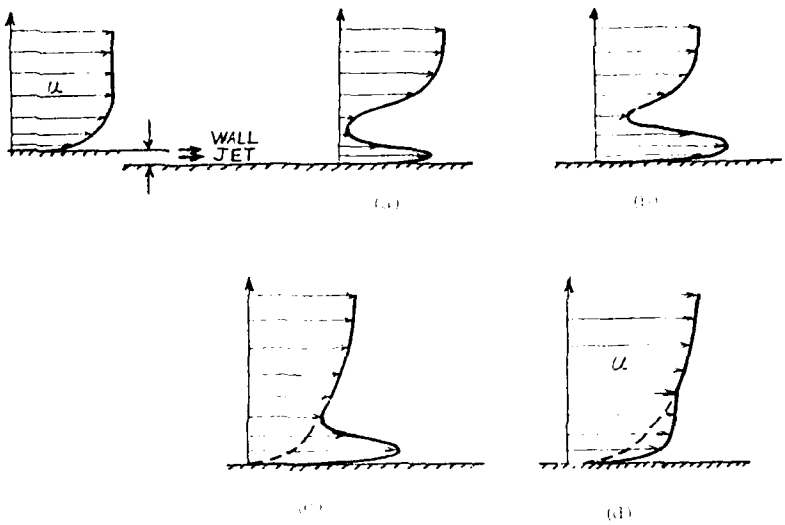

Fig. 5

Schematic of Turbulent Boundary Layer Development Downstream of a Wall Jet

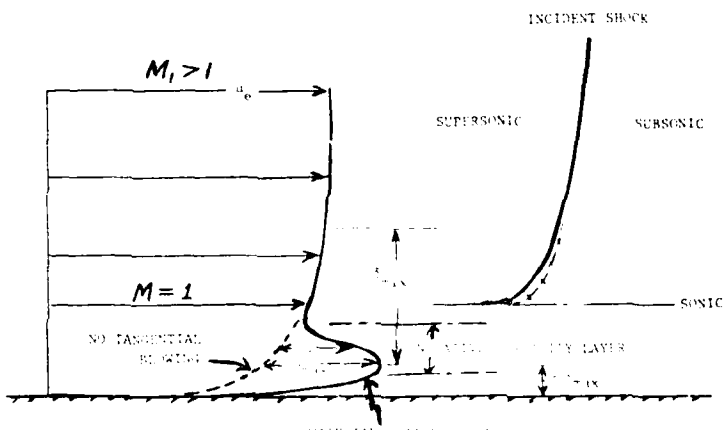

Fig. 6

Model for the Wall Jet-Effect on the Turbulent Boundary Layer Velocity Profile

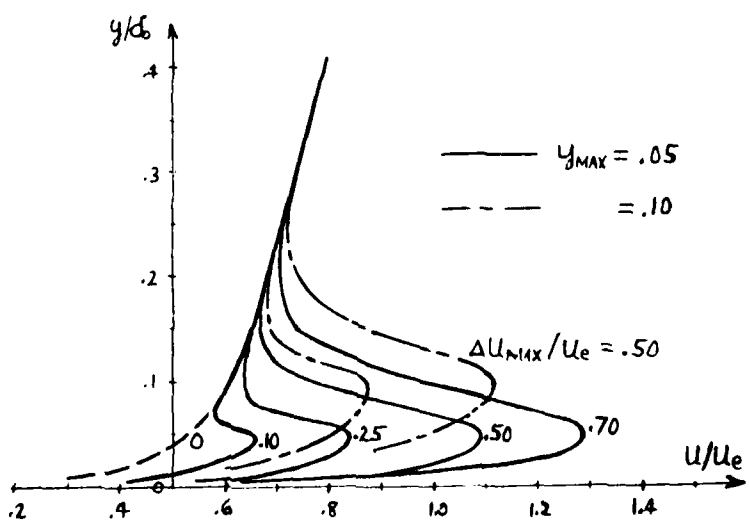

Fig. 7

Typical Turbulent Boundary Layer Profiles with Injection

$M_1 = 1.20$, $Re_{\delta^*} = 3.5 \times 10^4$
$H_{i_1} = 1.40$ (UNBLOWN)

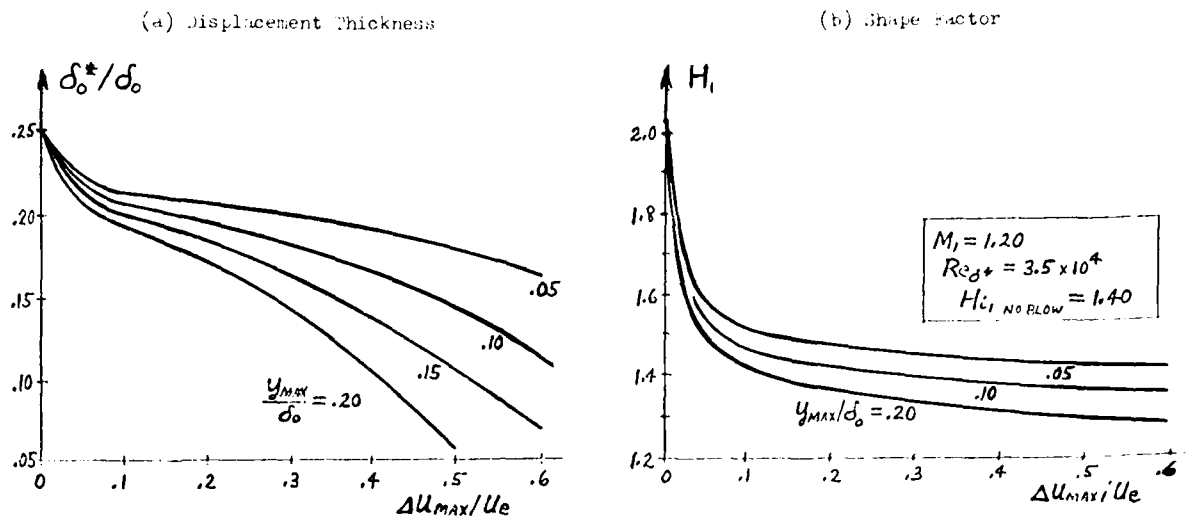

Fig. 8 Blowing Effect on Integral Properties of the Boundary Layer

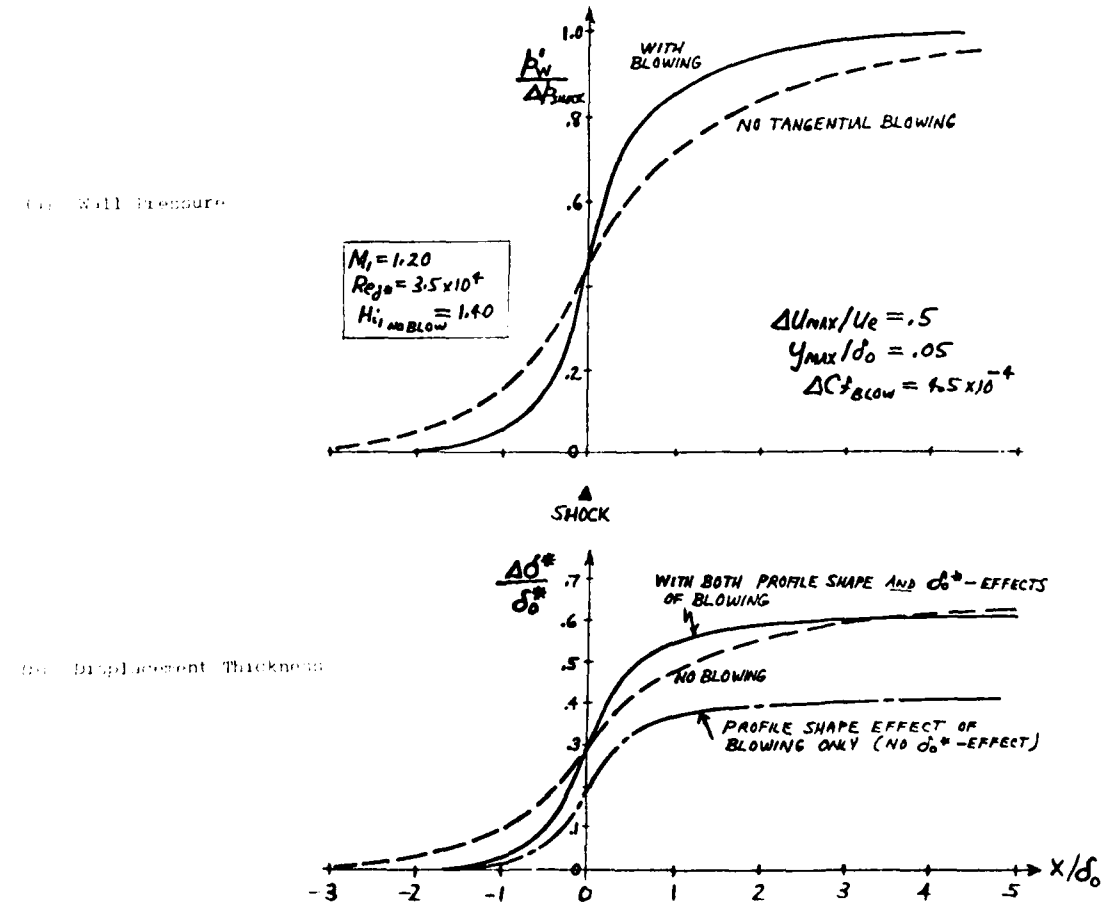

Fig. 9 Typical Blowing Effects on Interactive Property Distributions

(c) Skin Friction

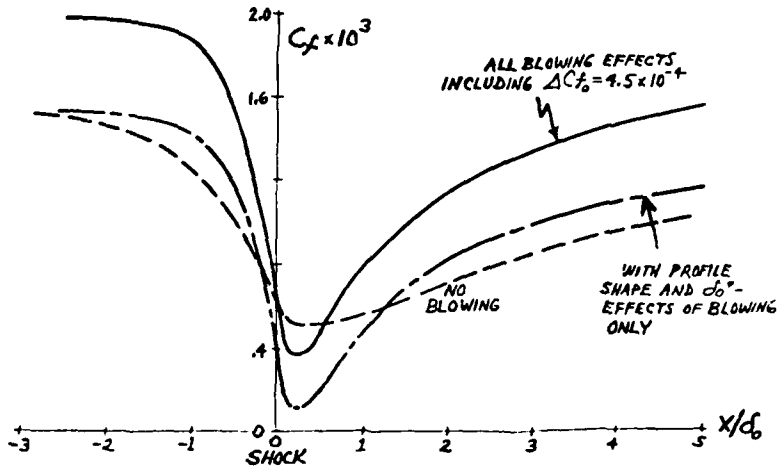

Fig. 9 (Continued)

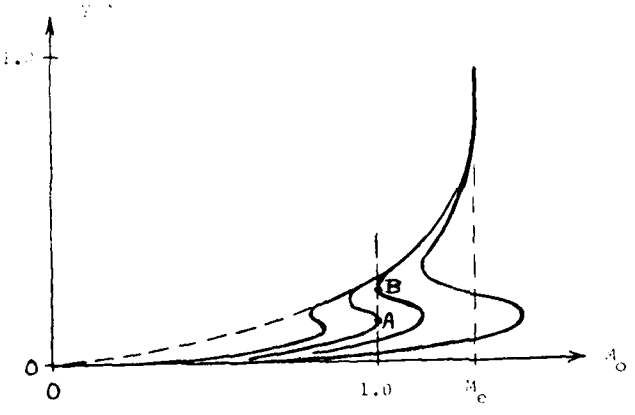

Fig. 10

Sonic and Supersonic Regions within a Blown Boundary Layer (Schematic)

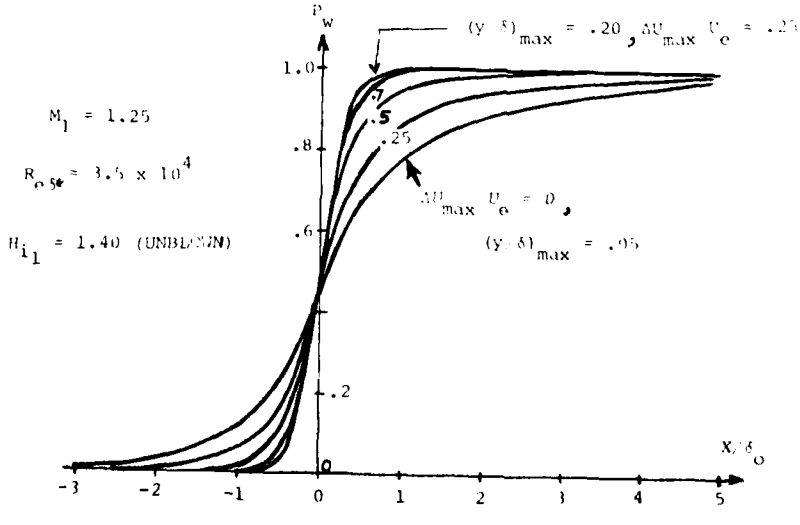

Fig. 11

Parametric Study of Wall Jet-Effect on Interaction Pressure Distribution

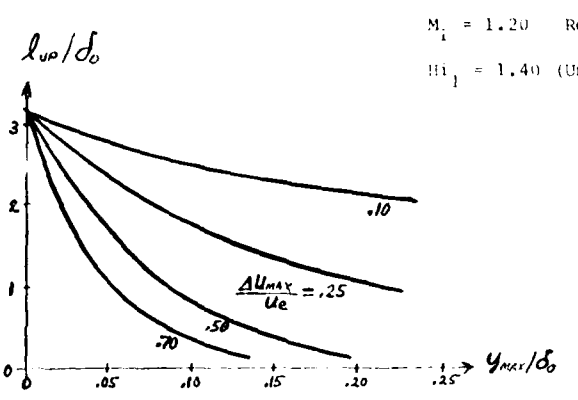

Fig. 12 Blowing Effect on Upstream Influence Distance

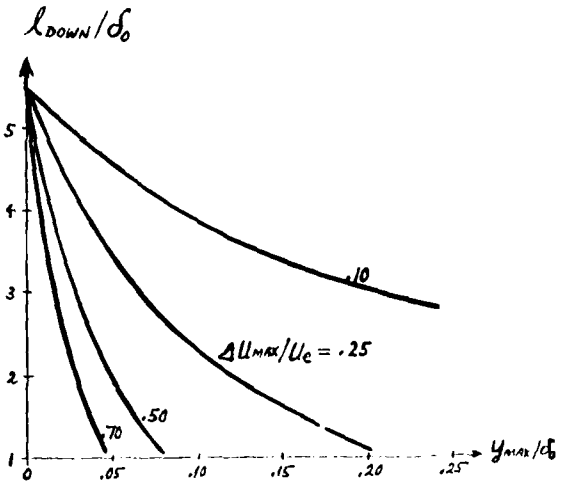

Fig. 13 Blowing Effect on Downstream Influence Distance

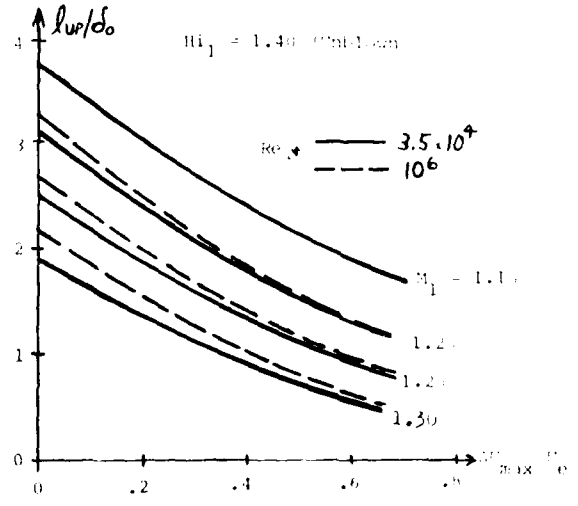

Fig. 14

Reynolds and Mach Number Effects on Blown Upstream Influence Distance

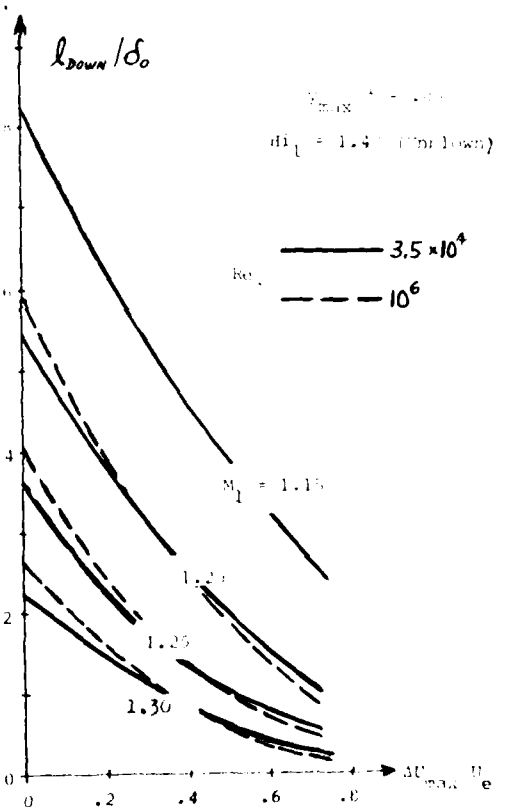

Fig. 15 Reynolds and Mach Number Effects on Blown Downstream Influence Distance

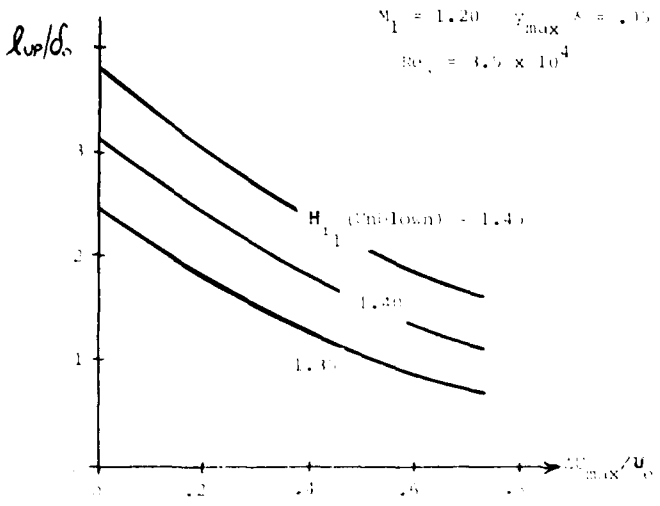

Fig. 16 Shape Factor Effect on Blown Upstream Influence

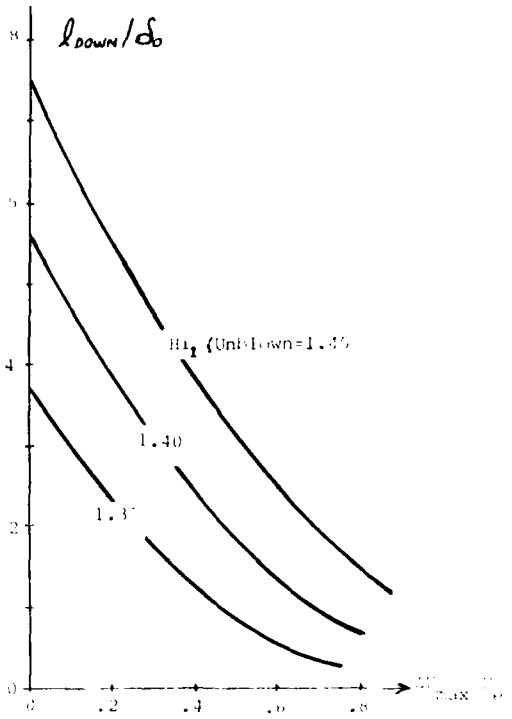

Fig. 17

Shape Factor Effect on Blown Downstream Influence

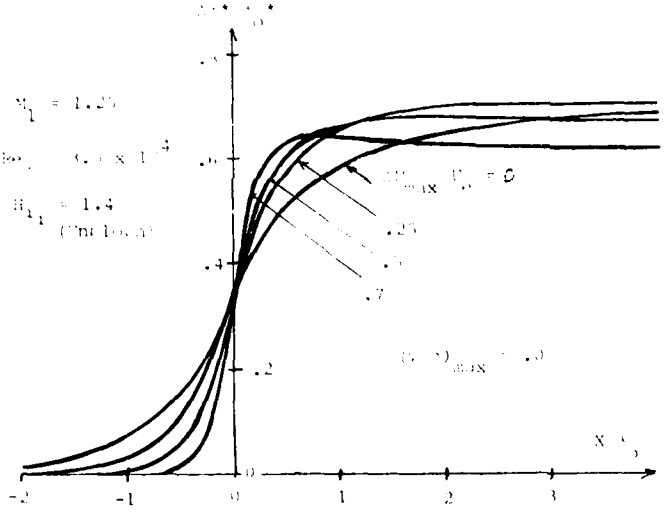

Fig. 18 Parametric Study of Wall Jet- Effect on Interactive Displacement Thickness Distribution

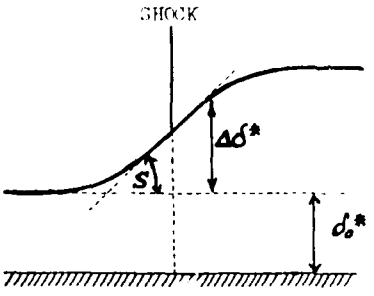

Fig. 19 Injection Effect on Viscous Wedge Angle

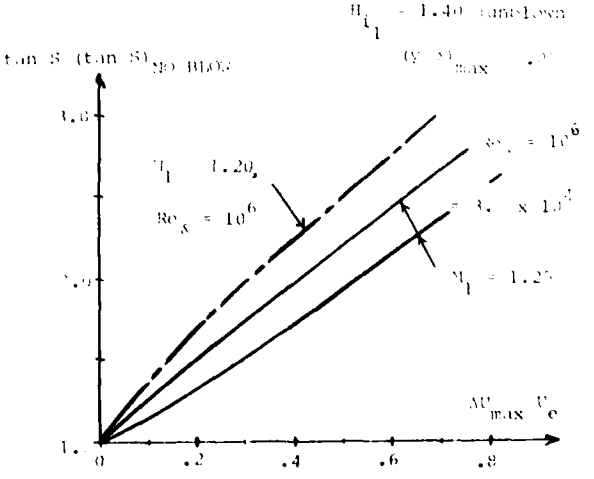

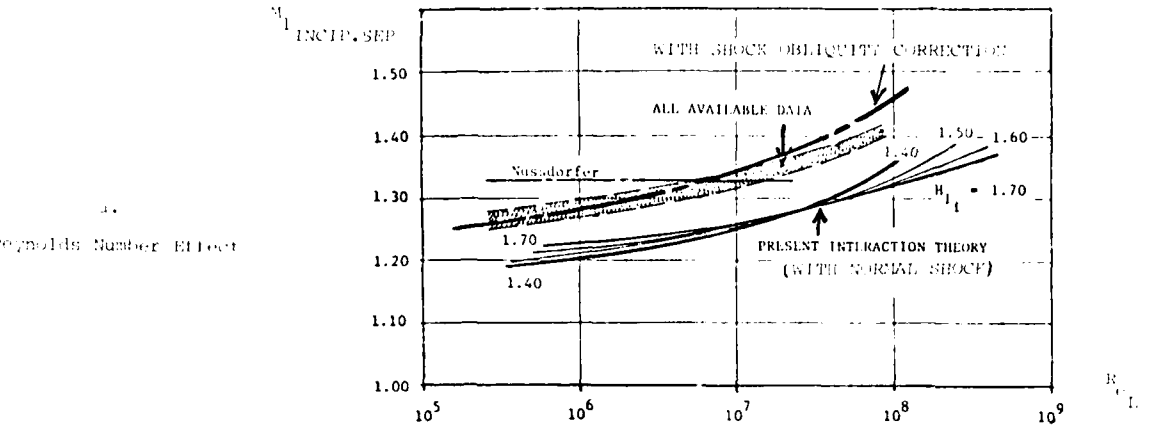

a.

Reynolds Number Effect

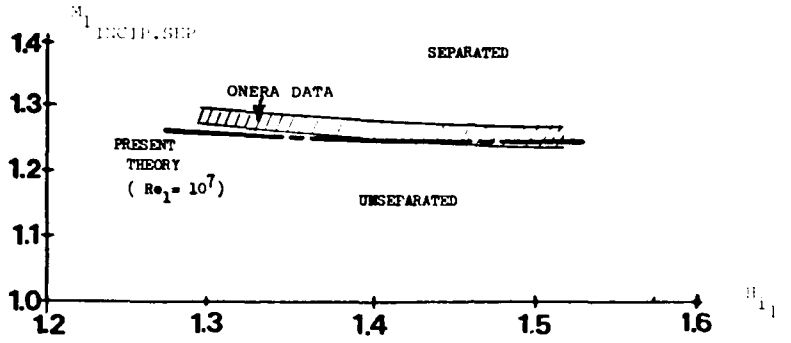

b.

Shape Factor Effect

Fig. 20 Mach Number for Incipient Separation at Shock Foot

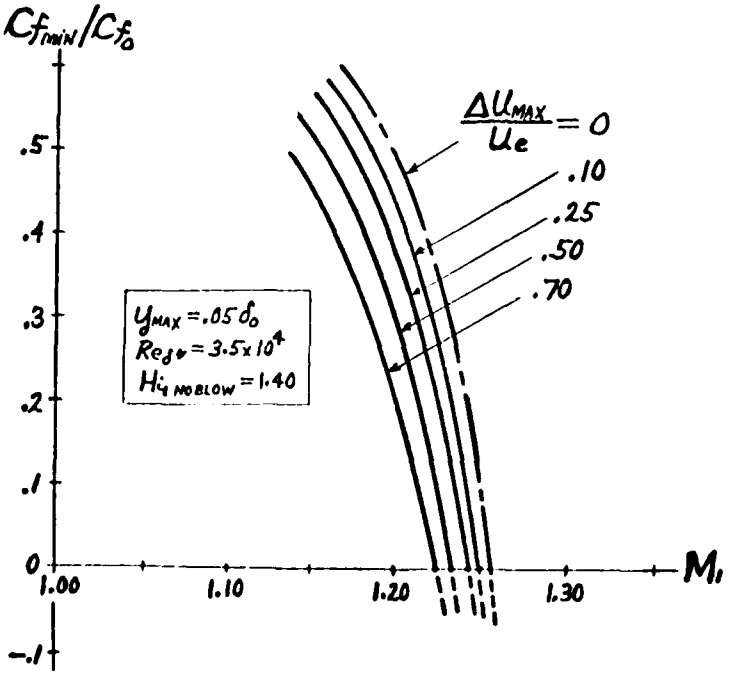

Fig. 21

Blowing Effect on Predicted Incipient Separation

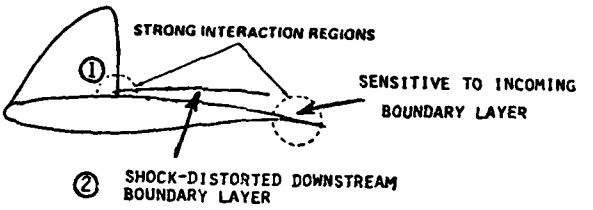

Fig. 22 Schematic of Global Viscous-Inviscid Interaction Problem on Supercritical Airfoils

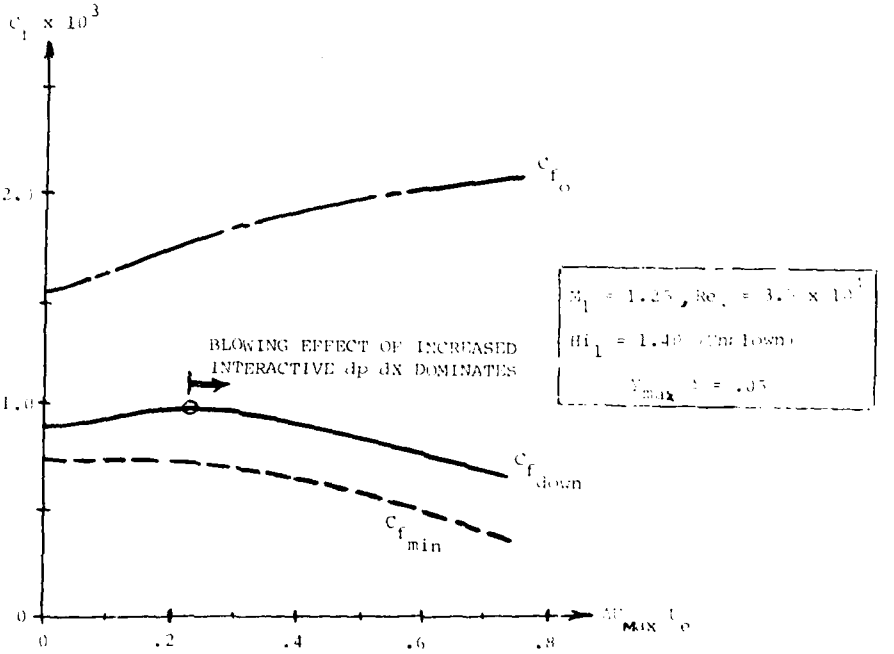

Fig. 23 Blowing Effects on Downstream Skin Friction Level


DA
FILM